

# Fault Tolerant Control of an Internal Combustion Engine Air Path using Super-Twisting Algorithm

Mohamed Guermouche\* Sofiane Ahmed Ali\*  
Nicolas Langlois\*

\* IRSEEM Technopôle du Madrillet 76801 Saint Etienne du Rouvray  
France Tel: +33 (0)2 32 91 58 85; e-mail: {mohamed.guermouche;  
sofiane.ahmedali; nicolas.langlois}@esigelec.fr

---

**Abstract:** In this paper, a passive fault tolerant control strategy carried out under the concept of higher order sliding mode control is developed for an internal combustion engine air path. The proposed fault tolerant strategy incorporates a Super-Twisting algorithm controller which handles parametric uncertainties and actuator faults. In this paper we consider two types of actuator faults, additive and loss-of-effectiveness faults. Theoretical results on the convergence of the proposed controller based on the Lyapunov theory are presented. The simulations of the proposed controller on a recently validated experimental air path engine model show good results under actuator faults conditions even in the presence of parametric uncertainties.

Keywords: Nonlinear control, Passive Fault-Tolerant Control (PFTC), Sliding Mode Control (SMC), Higher Order Sliding Mode Control (HOSMC), Super-Twisting Algorithm (STA), Internal Combustion Engine (ICE).

---

## 1. INTRODUCTION

Comparing to gasoline engines, diesel engines has the advantage of producing the requested torque under an optimal compromise between fuel consumption and given exhaust legislation emission level. To meet the requirements of emission standards EURO V and VI, the emissions of internal combustion engines, particularly Oxides of Nitrogen ( $NO_x$ ) and Particulate Matter (PM) must be controlled at every engine cycles. Earlier reduction mechanism suggested that  $NO_x$  emissions can be reduced by increasing the intake manifold Exhaust Gas Re-circulation (*EGR*) fraction, and smoke can be reduced by increasing the Air/Fuel Ratio (*AFR*) (Wahlström et al., 2010). The *EGR* and the *AFR* rates are controlled by the *EGR* and the Variable Geometry Turbine (*VGT*) actuators whose position determine the amount of the *EGR* flow in the intake manifold and thus, controls the *AFR* and the *EGR* ratios variables. The *VGT* and the *EGR* actuators are strongly coupled so that conventional calibration/mapping-based approaches, which uses traditional PI controllers faces difficulty to produce satisfactory and robust results in terms of torque responses, engine-out emissions at steady and transient state conditions, even with very time-consuming and detailed calibrations effort.

In the past decades, considerable research efforts have been dedicated to the control of modern internal combustion engines. Several controllers were proposed in the literature, e.g., Lyapunov control design (Jankovic and Kolmanovsky, 2000), robust gain-scheduled controller based on a Linear Parameter-Varying (LPV) model (Jung and Glover, 2006; Lihua et al., 2007; Xiukun and del Re, 2007), Indirect passivation (Larsen et al., 2000), predictive control (Ferreau et al., 2007) and Feedback linearization (Plianos et al., 2007; Dabo et al., 2009).

For the purpose of controlling the ICE, the authors in (Jankovic and Kolmanovsky, 2000) developed a full-7th order ICE model which describes the dynamics of several variables in the air path of the engine. To simplify the control design the seventh-order model is reduced to a third-order model which describes the dynamic of

the power of compressor and the pressures in the intake and the exhaust manifold. This simplification leads to the appearance of discrepancies between the description model and the real system due to the neglected dynamics, the model parametric uncertainties and the potential faults which can occur in the ICE air path.

In this paper, we deal with both model parametric uncertainties and engine actuator faults. In the ICE air path, model parametric uncertainties arise from variations in the engine cartographies, sources such as temperature change, and external or internal unmodelled disturbances. Engine actuator faults affect the ICE air path actuators. In this paper, we consider two types of actuator faults. The first one, model the faults as bounded additive periodic unknown signals that are superposed onto the control signal. The second one, consider the case of the loss of actuator effectiveness, modelled by a multiplicative factor that, when multiplied to the control signal, will reduce its effectiveness depending on the value of this factor.

Sliding Mode Control (SMC) which is known to perform well under parametric uncertainties and external disturbances (Utkin, 1977; Pisano and Usai, 2011) has become widespread and one of the most popular robust non-linear control method. In (Utkin et al., 2000; Upadhyay et al., 2002), the authors proposed a sliding mode based controllers which coordinates the *EGR* and the *VGT* actuator signals for the control of modern internal combustion engines. SMC Hybrid air path controllers for multiples combustion modes were also proposed in (Wang, 2008).

The main disadvantage of classic sliding mode control is the phenomenon of *chattering* which is characterized by the high frequency oscillations at the output of the system. In (Levant, 1993) the Higher Order Sliding-Mode control (HOSMC) was used in order to reduce or to eliminate the chattering phenomenon at high frequencies. Several algorithms to carry out HOSMC have been developed in the literature (see (Pisano and Usai, 2011) for a complete review). Among them, the Super-Twisting control algorithms (STA) require that the sliding variable be relative degree 1 with no need of the derivative of the sliding surface  $S$ . With its simplicity of implementation and

its power to eliminate the chattering phenomenon, STA algorithms are preferable over the classic sliding mode (Pisano and Usai, 2011), (Levant, 1993), (Gonzalez et al., 2011).

Comparing to the works in (Utkin et al., 2000; Upadhyay et al., 2002; Wang, 2008) the contribution of this paper consists in:

- Developing a passive STA controller centred on achieving fault tolerance for the ICE air path. The proposed controller is characterized by the simplicity of its structure. The controller handles both parametric uncertainties and actuator faults. Two types of actuator faults are treated simultaneously in this paper, additive actuator faults and loss-of-effectiveness. This is in our acknowledge the first time that those faults types are considered in the design of a ICE air path controller.
- The convergence of the proposed controller under the considered faults have been proved using strong Lyapunov function. Sufficient conditions on the controller gains had been derived providing robustness property, fault tolerance, and finite time convergence for the proposed controller.

This paper is organized as follows. Section II introduces the ICE air path modelling. Section III introduces the systems that we are dealing with, together with the assumptions required. The passive fault-tolerant STA based controller will be described in section IV. Simulation results are given in section V. Section VI summarizes conclusions and describes the future work.

## 2. CONSIDERED ICE AIR PATH MODEL

The schematic diagram of the ICE is shown in Fig. 1. At the top of the diagram we can see the turbocharger and the compressor mounted on the same shaft. The turbine delivers power to the compressor by transferring the energy from the exhaust gas to the intake manifold. Together, the mixture of air from the compressor and the exhaust gas from the *EGR* valve with the injected fuel burns, and produces the torque on the crank shaft.

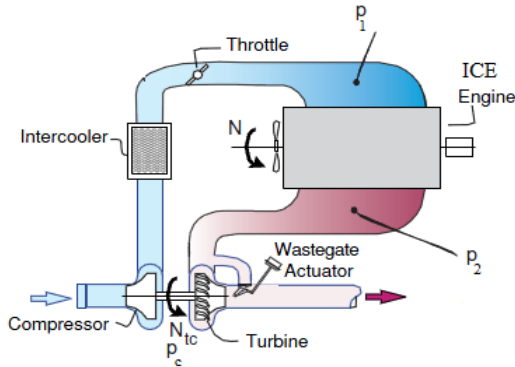


Fig. 1. Internal Combustion Engine

The full-order ICE model is a seventh-order one which contains seven states: intake and exhaust manifold pressure ( $p_1$  and  $p_2$ ), oxygen mass fractions in the intake and exhaust manifolds ( $F_1$  and  $F_2$ ), turbocharger speed ( $\omega_{tc}$ ) and the two states describing the actuator dynamics for the two control signals ( $u_1$  and  $u_2$ ).

In order to obtain a simple control law, and due to the fact that the oxygen mass fraction variables are difficult to measure, the seventh-order model is reduced to a third-order one (Jankovic and Kolmanovsky, 2000).

$$\begin{cases} \dot{p}_1 = k_1(W_c + W_{egr} - k_e p_1) + \frac{\dot{T}_1}{T_1} p_1 \\ \dot{p}_2 = k_2(k_e p_1 - W_{egr} - W_t + W_f) + \frac{\dot{T}_2}{T_2} p_2 \\ \dot{P}_c = \frac{1}{\tau}(\eta_m P_t - P_c) \end{cases} \quad (1)$$

where the compressor and the turbine mass flow rate ( $W_c$  and  $W_t$ ) are related to the compressor and the turbine power ( $P_c$  and  $P_t$ ) as follows:

$$W_c = P_c \frac{k_c}{p_1^\mu - 1} \quad (2)$$

and:

$$P_t = k_t(1 - p_2^{-\mu})W_t \quad (3)$$

Where:

$$k_c = \frac{\eta_c}{c_p T_a}, k_t = c_p \eta_t T_2, k_1 = \frac{R_a T_1}{V_1}, k_e = \frac{\eta_v N V_d}{R_a T_1}, k_2 = \frac{R_a T_2}{V_2}$$

Notice that the real inputs are the *EGR* and the *VGT* actuator openings. The considered inputs, in this case for the sake of simplicity, are  $u_1 = W_{egr}$  and  $u_2 = W_t$ , which are respectively the air flow through the *EGR* and the *VGT* actuators.

Since  $\dot{T}_1$  and  $\dot{T}_2$  have very slow variations (Jankovic and Kolmanovsky, 2000), their dynamic can be neglected. This yields the following simplified model:

$$\begin{cases} \dot{p}_1 = k_1(W_c + W_{egr} - k_e p_1) \\ \dot{p}_2 = k_2(k_e p_1 + W_f - W_{egr} - W_t) \\ \dot{P}_c = \frac{1}{\tau}(\eta_m P_t - P_c) \end{cases} \quad (4)$$

When replacing  $W_c$  and  $P_t$  by their expressions in (2) and (3), the simplified model can be expressed under the following control-affine form:

$$\dot{x} = f(x) + g_1(x)u_1 + g_2(x)u_2 \quad (5)$$

where  $x = (p_1, p_2, P_c)^T$  and

$$f(x) = \begin{bmatrix} k_1 k_c \frac{P_c}{p_1^\mu - 1} - k_1 k_e p_1 \\ k_2(k_e p_1 + W_f) \\ -\frac{P_c}{\tau} \end{bmatrix} \quad (6)$$

$$g_1(x) = \begin{bmatrix} k_1 \\ -k_2 \\ 0 \end{bmatrix}, g_2(x) = \begin{bmatrix} 0 \\ -k_2 \\ K_o(1 - p_2^{-\mu}) \end{bmatrix} \quad (7)$$

with  $K_o = \frac{\eta_m}{\tau} k_t$

We notice that the ICE model parameters ( $k_1, k_2, k_c, k_e, k_t, \tau, \eta_m$ ) have been identified under steady state conditions (i.e constant engine speed and constant fuelling rate) and extensive mapping. The nomenclature of the ICE parameters can be found in (Jankovic and Kolmanovsky, 2000).

## 3. SYSTEM FAULT DESCRIPTION

Here, we consider the class of non-linear system of the form:

$$\dot{x} = f(x) + g(x)u \quad (8)$$

Where  $x \in \mathbf{R}^n, u \in \mathbf{R}^m$  represent the state and the input vector respectively. The vector fields  $f$  and columns  $g$  are supposed to satisfy the classical smoothness assumptions with  $f(0) = 0$ . Adding to the previous classical assumptions, we assume that system (8) is affected by the following types of actuator faults.

*Assumption 1.* In this paper we assume two types actuator faults.

- An additive actuator fault enters the system in such a way that the faulty model can be written:

$$\dot{x} = f(x) + g(x)(u + F(x, t)) \quad (9)$$

where  $F(x, t)$  is bounded by an unknown positive constant  $D_m$  i.e

$$\|F(x, t)\| < D_m. \quad (10)$$

- The actuator loss-of-effectiveness is represented by a multiplicative matrix  $\alpha$  which affects the performance of each actuator in such a way that:

$$\dot{x} = f(x) + g(x)\alpha u \quad (11)$$

Where  $\alpha \in \mathbf{R}^{m \times m}$  is a diagonal continuous time varying matrix whose diagonal elements  $\alpha_{ii}, i = 1, \dots, m$ .

*Assumption 2.* We assume that the nominal system (8) is locally reachable (in the sense of (Vidyasagar, 1993), pp. 400, Definition 5)

Combining (9) and (11) the global faulty model of nominal system (8) can be written as follows:

$$\dot{x} = f(x) + g(x)(\alpha u + F(x, t)) \quad (12)$$

#### 4. FAULT-TOLERANT SUPER TWISTING CONTROLLER DESIGN FOR THE ICE AIR PATH

The proposed air path control strategy operates under the conventional combustion mode conditions (Wang, 2008). In this work the author suggested that for an optimal control performance, compressor mass flow  $W_c$  and Exhaust pressure manifold  $p_2$  are suitable choice for key output variable to be controlled. By a suitable change of coordinates, the authors in (Ahmed Ali et al., 2012) proposed to replace the compressor mass flow set-point ( $W_{cd}$ ) into an intake manifold pressure set-point ( $p_{1d}$ ). This transformation simplifies the control structure by defining new vector set-point ( $p_{1d}, p_{2d}$ ). The goal now, is to find a closed-loop controls which tracks these two variables.

Let us now consider system (1-7) and define the following two sliding surfaces  $S_1, S_2$

$$\begin{cases} S_1 = p_1 - p_{1d} \\ S_2 = p_2 - p_{2d} \end{cases} \quad (13)$$

The time derivative of  $S_1, S_2$  along the trajectories of system (5-7) leads to :

$$\begin{cases} \dot{S}_1 = k_1 W_c + k_1 u_1 - k_1 k_e p_1 - \dot{p}_{1d} \\ \dot{S}_2 = k_2 k_e p_1 + k_2 W_f - k_2 u_1 - k_2 u_2 - \dot{p}_{2d} \end{cases} \quad (14)$$

Now assume that the actuator faults described in (9) and (11) affect the VGT and the EGR actuators. Following (12), the faulty ICE air path model is rewritten as follows:

$$\begin{cases} \dot{S}_1 = k_1 W_c + k_1 \alpha_1 u_1 - k_1 k_e p_1 + k_1 F_1 - \dot{p}_{1d} \\ \dot{S}_2 = k_2 k_e p_1 + k_2 W_f - k_2 \alpha_1 u_1 - k_2 \alpha_2 u_2 - k_2 (F_1 + F_2) - \dot{p}_{2d} \end{cases} \quad (15)$$

Here  $(\alpha_1, \alpha_2)$ , characterize the amount of the loss-of-effectiveness model which affects the EGR and the VGT actuators.  $(F_1, F_2)$  characterize the additive faults which modifies the air flows through the EGR and the VGT actuators.

*Remarks 1.* The actuator loss-of-effectiveness  $\alpha_{1,2}$  in (15) characterize the actuator capability to achieve the control requirements. For example if  $\alpha_i = 1$ , we have a healthy actuator, if  $\alpha_i < 1$ , the actuator is working partially.

The control design will be achieved under the following assumptions.

*Assumption 3.* All the states of system (15) are available for measurements at every instant.

*Assumption 4.* To guarantee the local reachability of system (15), the additive faults  $F_1, F_2$  are uniquely time-dependent and  $(\alpha_{1,2} \neq 0)$  i.e  $0 < \epsilon \leq \alpha_{ii} \leq 1$

Consider now the faulty system (15) with the sliding manifold  $S = [S_1, S_2]^T$ . It is clear that the relative degree of  $S$  with respect to control inputs  $u = [u_1, u_2]^T$  is equal to 1. The dynamics of  $S$  takes the following form:

$$\dot{S} = A(X, F, P_1, X_d) + B(\alpha, P_2)u \quad (16)$$

Where  $X = [p_1, p_2, W_c]^T, F = [F_1, F_2]^T, P_1 = [k_1, k_2, k_e], X_d = [p_{1d}, p_{2d}]^T, \alpha = [\alpha_1, \alpha_2]^T, P_2 = [k_1, k_2]^T$  and

$$A = \begin{pmatrix} k_1 W_c - k_1 k_e p_1 + k_1 F_1 - \dot{p}_{1d} \\ k_2 k_e p_1 + k_2 W_f - k_2 (F_1 + F_2) - \dot{p}_{2d} \end{pmatrix}$$

$$B = \begin{pmatrix} \alpha_1 k_1 & 0 \\ -\alpha_1 k_2 & -\alpha_2 k_2 \end{pmatrix}$$

Introducing the variables  $x_1 = S_1, x_3 = S_2$ , system (16) is rewritten under the form:

$$\begin{cases} \dot{x}_1 = k_1 \alpha_1 u_1 + \xi_1(X, F, P_1, X_d) \\ \dot{x}_3 = -k_2 \alpha_2 u_2 + \xi_2(X, F, P_1, X_d, u_1) \end{cases} \quad (17)$$

Where:  $\xi_1(X, F, P_1, X_d) = k_1 W_c - k_1 k_e p_1 + k_1 F_1 - \dot{p}_{1d}$  and  $\xi_2 = k_2 k_e p_1 + k_2 W_f - k_2 (F_1 + F_2) - \dot{p}_{2d} - k_2 \alpha_1 u_1$ .

*Assumption 5.* The terms  $\xi_1$  and  $\xi_2$  are Lebesgue-measurable and uniformly bounded in any compact region of the state space  $x_1, x_3$  by  $\delta_1, \delta_2$  so that:

$$|\xi_1| < \delta_1 |x_1|^{\frac{1}{2}}, |\xi_2| < \delta_2 |x_3|^{\frac{1}{2}}$$

The task now is to design for system (17) a super-twisting controller which guarantee finite time convergence of the two sliding manifolds  $S_1, S_2$ . Following (Fridman and Levant, 2002) the proposed STA controller for system (17) takes the following form:

$$\begin{cases} u_1 = x_2 - \lambda_1 |x_1|^{1/2} \text{sign}(x_1) \\ \dot{x}_2 = -\lambda_2 \text{sign}(x_1) \\ u_2 = -x_4 + \lambda_3 |x_3|^{1/2} \text{sign}(x_3) \\ \dot{x}_4 = -\lambda_4 \text{sign}(x_3) \end{cases} \quad (18)$$

Where  $\lambda_i, \lambda_{i+1}, (i = 1, 3)$  satisfies the following conditions:

$$\begin{cases} \lambda_i > 2\delta_j \\ 2\varepsilon_j \lambda_{i+1} (\lambda_i - 2\delta_j) \geq \lambda_i (2(1 - \varepsilon_j) \frac{\lambda_{i+1}}{\lambda_i} + \frac{\delta_j}{2})^2 \quad (j = 1, 2) \\ \varepsilon_j = k_j \alpha_j \end{cases} \quad (19)$$

For  $(i, j) = (1, 1)$  and  $(i, j) = (3, 2)$

*Theorem 1.* Consider the uncertain faulty system (15). The passive fault tolerant STA controller (18) under conditions (19) ensure that the sliding manifolds  $[S_1, S_2]$  converges to zero in a finite time  $t(x_{i0})$

smaller than  $T = \frac{2V(x_{i0})^{\frac{1}{\nu}}}{\nu}$ , where  $V$  is the Lyapunov function defined in (21),  $\nu$  is a constant depending on the gains  $\lambda_i, \lambda_{i+1}, \varepsilon_j$  and  $\delta_j$ .

**Proof.** The proof of this theorem will be inspired from the Lyapunov function defined by the authors in (Moreno and Osorio, 2008). Applying the control law (18) in (17) leads to the following differential inclusions which are understood in the Filippov sense (Filippov, 1988):

$$\begin{cases} \dot{x}_1 = -k_1 \alpha_1 \lambda_1 |x_1|^{1/2} \text{sign}(x_1) + k_1 \alpha_1 x_2 + \xi_1(X, F, P_1, X_d) \\ \dot{x}_2 = -\lambda_2 \text{sign}(x_1) \\ \dot{x}_3 = -k_2 \alpha_2 \lambda_3 |x_3|^{1/2} \text{sign}(x_3) + k_2 \alpha_2 x_4 + \xi_2(X, F, P_1, X_d, u_1) \\ \dot{x}_4 = -\lambda_4 \text{sign}(x_3) \end{cases} \quad (20)$$

Let us now consider for each subsystems  $(x_1, x_2)$  and  $(x_3, x_4)$  the following Lyapunov function (Moreno and Osorio, 2008):

$$V_i = X_i^T P_i X_i \quad (i = 1, 3) \quad (21)$$

where:

$$X_i^T = [|x_i|^{\frac{1}{2}} \text{sign}(x_i), x_{i+1}] \quad (22)$$

and:

$$P_i = \frac{1}{2} \begin{pmatrix} 4\lambda_{i+1} + \lambda_i^2 & -\lambda_i \\ -\lambda_i & 2 \end{pmatrix} \quad (23)$$

We notice that  $V_i$  is continuous but not differentiable at  $x_i = 0$ . Moreover, it is positive and radially unbounded for  $\lambda_{i+1} > 0$ . Differentiating  $V_i$  with respect to time yields to:

$$\dot{V}_i = \dot{X}_i^T P X_i + X_i^T P \dot{X}_i \quad (24)$$

Taking the time derivative of (22) along the trajectories of (20), we derive:

$$\dot{X}_i = \frac{1}{|x_i|^{\frac{1}{2}}} (A_i X_i + B_j^T) \quad (25)$$

Where:

$$A_i = \begin{pmatrix} \frac{-\varepsilon_j \lambda_i}{2} & \frac{\varepsilon_j}{2} \\ -\lambda_{i+1} & 0 \end{pmatrix} \quad (26)$$

and

$$B_j = \left( \frac{\xi_j}{2}, 0 \right) \quad (27)$$

Combining (24-27) yields:

$$\dot{V}_i = -\frac{1}{|x_i|^{\frac{1}{2}}} X_i^T Q_i X_i + \frac{1}{|x_i|^{\frac{1}{2}}} \xi_j q_i^T X_i \quad (28)$$

where:

$$Q_i = \begin{pmatrix} \frac{\varepsilon_j \lambda_i (4\lambda_{i+1} + \lambda_i^2)}{2} - \lambda_i \lambda_{i+1} & \star \\ \frac{2\lambda_{i+1} (1 - \varepsilon_j) - \varepsilon_j \lambda_i^2}{2} & \frac{\varepsilon_j \lambda_i}{2} \end{pmatrix} \quad (29)$$

and

$$q_i^T = [2\lambda_{i+1} + \frac{\lambda_i^2}{2}, -\frac{\lambda_i}{2}] \quad (30)$$

Taking into account the perturbation bounds in assumption 5 then :

$$\frac{1}{|x_i|^{\frac{1}{2}}} \xi_j q_i^T X_i \leq \frac{1}{|x_i|^{\frac{1}{2}}} \delta_j X_i^T \Delta_i X_i \quad (31)$$

Where:

$$\Delta_i = \begin{pmatrix} 2\lambda_{i+1} + \frac{\lambda_i^2}{2} & -\frac{\lambda_i}{4} \\ -\frac{\lambda_i}{4} & 0 \end{pmatrix} \quad (32)$$

The derivative of the Lyapunov function can be rewritten as follows:

$$\dot{V}_i = -\frac{1}{|x_i|^{\frac{1}{2}}} X_i^T \tilde{Q}_i X_i \quad (33)$$

Where:

$$\tilde{Q}_i = \frac{\lambda_i}{2} \begin{pmatrix} 4\varepsilon_j \lambda_{i+1} + \varepsilon_j \lambda_i^2 - 2\lambda_{i+1} - (4\frac{\lambda_{i+1}}{\lambda_i} + \lambda_i) \delta_j & \star \\ 2(1 - \varepsilon_j) \frac{\lambda_{i+1}}{\lambda_i} - \varepsilon_j \lambda_i + \frac{\delta_j}{2} & \varepsilon_j \end{pmatrix} \quad (34)$$

$\dot{V}_i$  is negative if  $\tilde{Q}_i > 0$ , and it is easy to see that this is the case if the gains are as in (19). Since  $V_i$  is positive and radially unbounded, it satisfies the following well-known property:

$$\Pi_{min}(P_i) \|X_i\|^2 \leq V_i \leq \Pi_{max}(P_i) \|X_i\|^2 \quad (35)$$

Where  $\|X_i\|^2 = |x_i| + x_{i+1}^2$  denotes the Euclidean norm of  $X_i$ , and  $\Pi_{min}(P_i)$ ,  $\Pi_{max}(P_i)$  are the minimum and maximum eigenvalues of the matrix  $P_i$ . From (33) we derive:

$$\dot{V}_i \leq -\frac{1}{|x_i|^{\frac{1}{2}}} \Pi_{min}(\tilde{Q}_i) \|X_i\|^2 \quad (36)$$

After a simple computation (see (Moreno and Osorio, 2008)), we have:

$$\dot{V}_i \leq -\nu V_i^{\frac{1}{2}} \quad (37)$$

Where

$$\nu = \frac{\Pi_{min}^{\frac{1}{2}}(P_i) \Pi_{min}(\tilde{Q}_i)}{\Pi_{max}(P_i)}$$

Integrating (37) yields that  $x_i$  converges toward zero in finite time at most after  $T = \frac{2V(x_{i0})^{\frac{1}{2}}}{\nu}$ , this complete the proof.

## 5. SIMULATION AND EVALUATION

In this section, we report numerical results obtained from the simulation of controller (18) on the reduced third order model developed in (1-7). Numerical simulations were performed in real-time Software In the Loop (SIL) using the dSpace modular simulator. This real-time platform is based on the DS-1006 board interfaced with Matlab/Simulink software. The engine used is a common rail direct-injection in-line-4-cylinder provided by a French manufacturer. Numerical values of  $(\eta_t, \eta_c, \eta_v, \eta_m)$  cartographies in the ICE model were provided by the manufacturer. The model parameters nominal values  $k_{o1}, k_{o2}, k_{oc}, k_{oe}, k_{ot}, \tau_o, \eta_{om}$  and  $\mu_o$  are usually identified around some given operating points. In these simulations, the parameters of the model (1-7) were taken from (Larsen et al., 2000) i.e ( $k_{o1}=143.91, k_{o2}=1715.5, k_{oc}=0.0025, k_{oe}=0.028, k_{ot}=391.365, \tau_o=0.15, \eta_{om}=0.95, \mu_o=0.285$ ). To avoid the chattering associated with sliding motion, a well-known continuous approximation of the function  $sign(S)$  is given by:

$$Sign(S) = \frac{s}{|s| + \xi} \quad (38)$$

This approximation is used to ensure that the sliding motion will be in the vicinity of the line ( $S = 0$ ). In this simulation the approximation of the  $sign$  function has been implemented with  $\xi = 0.01$ . Moreover the sampling step time for all the simulations is the same,  $10^{-4}$ s. To demonstrate the efficiency of our proposed controller, a comparison is performed between the STA controller and the Adaptive Integral Sliding Mode Controller (AISMC) proposed by the authors in (Guermouche et al., 2013). In this work the authors demonstrated that AISMC controller with an adaptation gain mechanism, ensures that the sliding manifolds  $[S_1, S_2]$  converges asymptotically toward zero.

For the AISMC controller,  $\gamma_1, \gamma_2$ , governs the dynamic of the discontinuous adaptive control gains, while  $\rho_1, \rho_2$  characterize the level of the integral action wanted by the user for a given control requirements. Comparing to the work of the authors in (Guermouche et al., 2013), the advantages of the proposed STA controller are :

- The convergence of the STA controller is finite time while the AISMC one is asymptotic.
- The STA control structure is less consuming in terms of computational complexity comparing to the AISMC one.

In this simulation, we assume certain uncertainties on the set of the ICE model parameters  $P=(k_1, k_2, k_c, k_e, k_t, \tau, \eta_m, \mu)$ . To make it simple, additive uncertainties are considered in this simulation, i.e for a nominal value  $P_{oi}(1 \leq i \leq 8)$ , the considered  $P_i$  in the simulation takes the following form:

$$P_i \subset P, P_i = P_{oi} + \delta P_{oi}$$

Where  $\delta P_{oi}$  represent the maximum value of the uncertainty on the considered model parameter.

The performances of the AISMC and the STA controllers are compared when both additive time varying faults and loss-of effectiveness actuators faults affects the EGR and the VGT actuators. The goal here was to evaluate the performance of each controller in terms of tracking error and chattering effects. These performances are summarised in Table 2. where an RMS (Root Mean Square) value, quantifies for each case, the Control Effort (CE) of the EGR and the VGT actuator and the Tracking Error (TE) of the controlled output  $W_c$  and  $p_2$ . Finally the simulations were conducted under the control requirements defined in Table 1.:

Table 1. Control requirements for the AISMC and the STA controllers

variable	Setpoint1	Setpoint 2
$W_{cd}$ (Kg/s)	0.03	0.05
$P_{2d}$ (Bar)	1.45	1.75
$W_f$ (Kg/h)	3	7

5.1 Case 1: Additive leakage time varying faults and multiplicative loss-of-effectiveness time varying faults in EGR and VGT actuators with 20% parametric uncertainties

In this case, we evaluate the performance of the AISMC and the STA controllers by considering both of additive and multiplicative time varying faults (leakage and loss-of-effectiveness) added to 20% parametric uncertainties. We consider a fault scenario where:

- At t=25 s, the additive leakage time varying fault  $F(t)$  witch affect the VGT and the EGR actuators, takes the following form:

$$F(t) = \begin{cases} 0 \times (1, 1)^T & \text{if } t < 25s \\ -0.05 + 0.02 \sin(0.2\pi t) \times (1, 1)^T & \text{if } t \geq 25s \end{cases}$$

- At t=55 s, the multiplicative loss-of-effectiveness time varying fault occurs in the EGR and the VGT actuators following this model:

$$\alpha(t) = \begin{cases} I_{2 \times 2} & \text{if } t < 55s \\ 0.2 + 0.05 \sin(0.2\pi t) \times I_{2 \times 2} & \text{if } t \geq 55s \end{cases}$$

In this simulation, the gains of controllers were kept in the same manner as in the case 1,  $\lambda_1, \lambda_2, \lambda_3, \lambda_4=[0.3, 0.3, 0.3, 0.3]$  and  $\gamma_1, \gamma_1, \rho_1, \rho_2=[1, 50, 300, 300]$ .

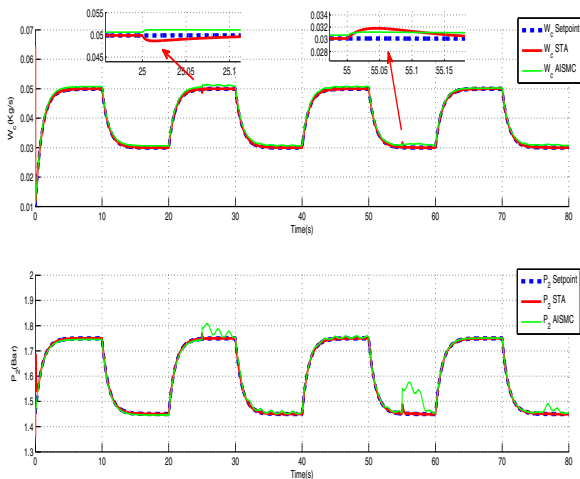


Fig. 2.  $W_c$  and  $p_2$  tracking performance for the STA and the AISMC with additive time varying fault and actuators loss-of-effectiveness and 20 % parametric uncertainties

Fig. 2. shows the performances of the STA and the AISMC controllers when both time varying additive and loss-of-effectiveness actuators faults occurs in the ICE. We can observe that the two controllers exhibits an oscillatory behaviour starting from t=25s with a significant magnitude and high frequency, specially for the AISMC. After t=55s, we also observe a random behaviour with some peaks of divergence that the controllers try to reduce but still unable to completely eliminate. This is confirmed looking to Table 2. where the RMS of TE is increased.

Table 2. RMS of Tracking Error (TE) and Control Effort (CE)

	Control Algorithm	RMS of CE EGR	RMS of CE VGT	RMS of TE ( $W_c$ )	RMS of TE ( $P_2$ )
Case 1	STA	0.0288	0.1283	3.4470e-004	0.0117
	AISMC	0.0294	0.1329	0.0013	0.0126
Case 2	STA	0.0386	0.1316	1.3252e-004	5.3214e-004
	AISMC	0.0462	0.1347	2.1594e-004	0.0054

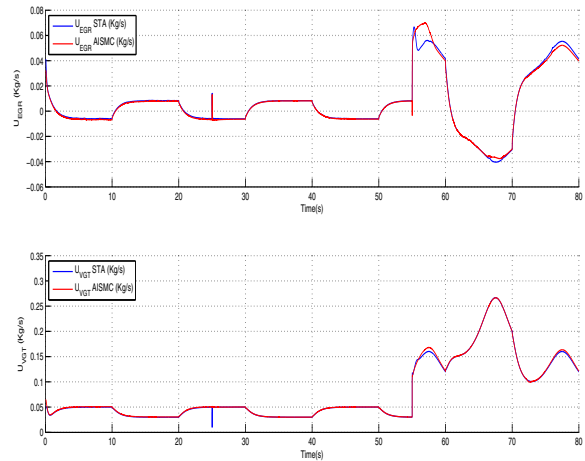


Fig. 3. Control inputs  $U_{EGR}$  and  $U_{VGT}$  for the STA and the AISMC additive time varying fault and actuators loss-of-effectiveness and 20 % parametric uncertainties

The Control efforts for both controllers have increased in this case. Indeed, in Fig. 3. we can see that both of te STA and AISMC controllers tried to compensate the leakage at t=25s and the loss-of-effectiveness at t=55s.

5.2 Case 2: Additive leakage time varying faults and multiplicative loss-of-effectiveness time varying faults in EGR and VGT actuators with 20% parametric uncertainties with increased gains

To remedy the problems of robustness and fault tolerance found in case 1, we increase the controllers gains. So we consider the same fault scenario in case 1 but with changing the STA gains to  $\lambda_1, \lambda_2, \lambda_3, \lambda_4=[3, 3, 3, 3]$  and the AISMC gains to  $\gamma_1, \gamma_1, \rho_1, \rho_2=[50, 950, 4500, 8500]$ .

We can see from Fig. 4. that performances of the STA controller have been considerably improved. The leakage (additive time varying faults) and the actuator loss-of-effectiveness (multiplicative time varying faults) are completely rejected from the states trajectories by the STA controller. For the AISMC controller, we can see that the magnitude of oscillations observed in case 1 is reduced thanks to the integral action and control gains but still not enough to reach the same level of performances comparing to the STA controller. Indeed, the RMS of TE  $W_c$  and  $p_2$  for the STA controller are smaller than the AISMC one (Table 2.).

We note from Fig. 5. that the oscillatory behaviour of controls efforts ( $U_{egr}, U_{vgt}$ ) has been considerably reduced. For the AISMC, this is due to the increase of integral action and for the STA, its due to the well known properties of reduction of chattering effect.

6. CONCLUSIONS AND FUTURE WORK

In this paper, a fault-tolerant STA controller is designed for controlling the ICE air path. Numerical simulations shows that the proposed controller is fault-tolerant for the different types of actuator faults considered in this paper. Comparing to the AISMC controller

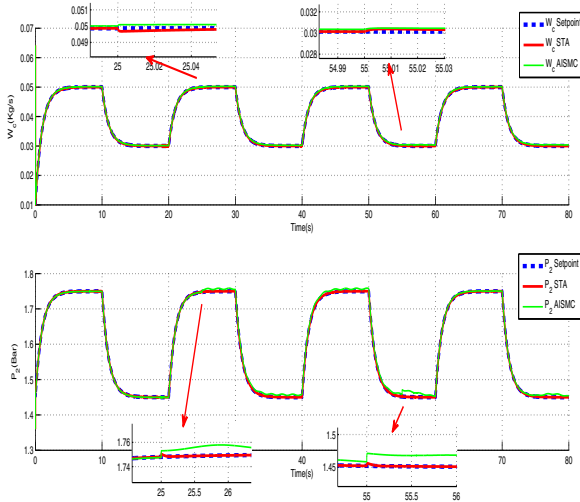


Fig. 4.  $W_c$  and  $p_2$  tracking performance for the STA and the AISMC with additive time varying fault and actuators loss-of-effectiveness and 20 % parametric uncertainties with increased gains

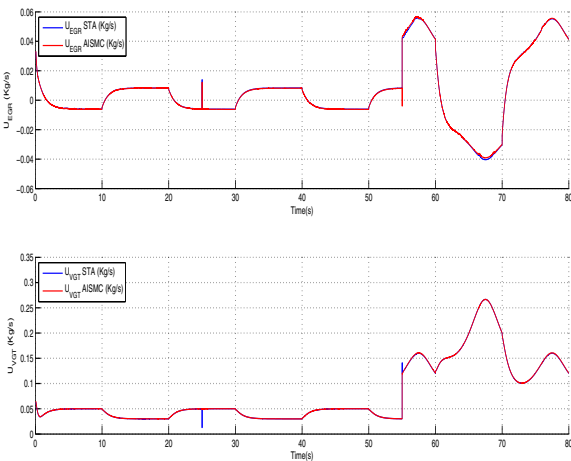


Fig. 5. Control inputs  $U_{EGR}$  and  $U_{VGT}$  for the STA and the AISMC additive time varying fault and actuators loss-of-effectiveness and 20 % parametric uncertainties with increased gains

the STA controller is characterized by the simplicity of its control structure. Indeed, the AISMC controller is based upon the tuning of 4 control parameters. It turns out from the simulation results that improving the performance of the AISMC controller needs always a compromise between those 4 parameters. For the STA controller the control parameters have been easily modified in the simulation and the tracking performances were clearly better than the AISMC ones. In our future works we intend to improve the performance of the proposed STA controller by designing an adaptive super twisting version of this algorithm. As it was the case for the AISMC, the control gains will be automatically tuned without knowing the bounds of the uncertainties and the failures affecting this controller.

ACKNOWLEDGEMENTS

The authors gratefully thank Région Haute Normandie OSEO and FEDER for financially supporting this work and its forthcoming application to an ICE control within the framework of the VIRTUOSE project

REFERENCES

S. Ahmed Ali, B. N'doye, and N. Langlois. Sliding mode control for turbocharged diesel engine. *International Conference on Control and Automation (MED)*, pages 996–1001, 2012.

M. Dabo, N. Langlois, and H. Chafouk. Dynamic feedback linearization applied to asymptotic tracking: Generalization about the turbocharged diesel engine outputs choice. *IEEE American Control Conference*, pages 3458–3463, 2009.

H.J. Ferreau, P. Ortner, P. Langthaler, L. del Re, and M. Diehl. Predictive control of a real-world diesel engine using extended online active set strategy. *Annual Review in Control*, 31:293–301, 2007.

A. F. Filippov. Differential equations with discontinuous right-hand sides. *Dordrecht, The Netherlands: Kluwer*, 1988.

L. Fridman and A. Levant. Higher order sliding modes. *Sliding Mode Control in Engineering, Ch. 3, Marcel Dekker, Inc*, pages 53–101, 2002.

T. Gonzalez, J.A. Moreno, and L. Fridman. Variable gain super-twisting sliding mode control. *IEEE Transactions on Automatic Control*, 2011.

M. Guermouche, S. Ahmed Ali, and N. Langlois. An adaptive integral sliding mode control design for internal combustion engine air path. *1st IFAC Workshop on Advances in Control and Automation Theory for Transportation Applications*, pages 87–94, 2013.

M. Jankovic and I. Kolmanovsky. Constructive lyapunov control design for turbocharged diesel engines. *IEEE Transactions on Control Systems Technology*, 8:288–299, 2000.

M. Jung and K. Glover. Calibration linear parameter-varying control of a turbocharged diesel engine. *IEEE Transactions on Control Systems Technology*, 14:45–62, 2006.

M. Larsen, Jankovic M, and P.V. Kokotovic. Indirect passivation design for diesel engine model. *IEEE International Conference application*, 2000.

A. Levant. Sliding and sliding accuracy in sliding mode control. *International Journal of Control*, 58, 1993.

L. Lihua, W. Xiukun, and L. Xiaohu. Lpv control for the air path system of diesel engines. *IEEE International Conference Control and Automation ICCA*, pages 873–878, 2007.

J. Moreno and M. Osorio. A lyapunov approach to second-order sliding mode controllers and observers. *IEEE Conference on Decision and Control*, pages 2856–2861, 2008.

A. Pisano and E. Usai. Sliding mode control: A survey with application in math. *Mathematics and Computers in Simulation*, 81:954–979, 2011.

A. Plianos, A. Achir, R. Stobart, N. Langlois, and H. Chafouk. Dynamic feedback linearization based control synthesis of the turbocharged diesel engines. *IEEE American Control Conference*, pages 4407–4412, 2007.

D. Upadhyay, V.I. Utkin, and G. Rizzoni. Multivariable control design for intake flow regulation of a diesel engine using sliding mode. *In Proceedings of the 15th Triennial IFAC World Congress*, pages 1389–1394, 2002.

V. I. Utkin, H.-C. Chang, I. Kolmanovsky, and J. A. Cook. Sliding mode control for variable geometry turbocharged diesel engines. *IEEE American Control Conference*, pages 584–588, 2000.

V.I. Utkin. Variable structure systems with sliding mode: A survey. *IEEE Transactions of Automatic Control*, 22(5):212–222, 1977.

M. Vidyasagar. Nonlinear systems analysis. *2nd ed. Englewood Cliffs, NJ: Prentice-Hall*, 1993.

Johan Wahlstrm, Lars Eriksson, and Lars Nielsen. Egr-vgt control and tuning for pumping work minimization and emission control. *IEEE Transactions on Control Systems Technology*, 18(4):993–1003, 2010.

J. Wang. Hybrid robust air-path control for diesel engines operating conventional and low temperature. *IEEE Transactions on Control Systems Technology*, 16:1138–1151, 2008.

W. Xiukun and L. del Re. Gain scheduled  $h_\infty$  control for air path systems of diesel engines using lpv techniques. *IEEE Transactions on Control Systems Technology*, 15:406–415, 2007.